CHAPTER 3

DOUBLE RELAXATION TIMES, DIPOLE MOMENTS, ENERGY PARAMETERS AND MOLECULAR STRUCTURES OF SOME APROTIC POLAR MOLECULES FROM RELAXATION PHENOMENA

3.1. Introduction :

The absorption of high frequency electric energy by aprotic polar liquids in nonpolar solvents has attracted much attention [3.1-3.2]. Such liquids have wide biological applications and act as building blocks of proteins and enzymes because of their high values of dielectric constants. They showed weak molecular association of monomer or dimer formation under *X*-band (~10 GHz) electric field. Many workers [3.3-3.4] studied their structural and associational aspects in high frequency (*f*) electric field by using the concentration variation method of Gopalakrishna [3.5]. However no attempt has been made so far to observe their double relaxation phenomena in nearly 10 GHz electric field, which seems to be the most effective dispsersive region [3.6] for them.

We, therefore, measured real ε_{ij}' and imaginary ε_{ij}'' parts of complex dielectric constant ε_{ij}^* of liquids (j) like dimethylsulphoxide (DMSO) at 25^0, 30^0, 35^0 and 40^0C; N,N-diethylformamide (DEF) at 30^0C; N,N-dimethylformamide (DMF) and N,N-dimethylacetamide(DMA) at 25^0C in benzene (i) at nearly 10 GHz electric field by a Hewlett Packard Impedance Analyser 4192A together with the static and infinite frequency dielectric constants ε_{oij} (at 1 KHz) and $\varepsilon_{\infty ij}$ $(=n_{Dij}^2)$ by Abbe's refractometer within 1% accuracy [3.7-3.8]. The measured data of Table 3.1 were used to detect their possible existence of double relaxation phenomena by the recently developed single frequency measurement [3.9-3.10] method.

The relaxation times τ_2 and τ_1 due to end over end rotation for the whole molecule as well as its flexible part attached to the parent one were obtained from the slope and intercept of a derived linear equation of $(\varepsilon_{oij}-\varepsilon_{ij}')/(\varepsilon_{ij}'-\varepsilon_{\infty ij})$ with $\varepsilon_{ij}''/(\varepsilon_{ij}'-\varepsilon_{\infty ij})$ as seen graphically in Fig.3.1 for different weight fractions w_j of solutes [3.9-3.10]. The intercepts and slopes of the linear curves of Fig.3.1 together with % of errors in terms of correlation coefficients '*r*' are placed in Table 3.2. τ_1 in Table 3.2 is very close to reported τ [3.5]. The relative contributions c_1 and c_2 towards dielectric relaxation due to τ_1 and τ_2 are calculated from the values of $x=(\varepsilon_{ij}'-\varepsilon_{\infty ij})/(\varepsilon_{oij}-\varepsilon_{\infty ij})$ and $y=\varepsilon_{ij}''/(\varepsilon_{oij}-\varepsilon_{\infty ij})$ at $w_j \rightarrow 0$ from their respective plots with w_j's in Figs.3.2 and 3.3 respectively. The estimated values of c_1 and c_2 together with those from Fröhlich's equations [3.11-3.12] are presented in Table3.3 for comparison.

The dipole moments μ_2 and μ_1 of the whole and the flexible part attached to the parent molecule due to τ_2 and τ_1 in terms of slopes β of high frequency conductivities σ_{ij} against w_j's [3.13] of Fig.3.4 were estimated to present in Table 3.4. The variation of μ_2 and μ_1 of DMSO with temperature and the estimated thermodynamic energy parameters from $\ln(\tau_2 T)$ and $\ln(\tau_1 T)$ against $1/T$ respectively supports the rotation of flexible parts of molecule under GHz electric field. We have also calculated the static experimental parameter X_{ij} involved with ε_{oij} and n_{Dij}^2 at different

Table 3.1: Concentration variation of dielectric relaxation parameters like real part of dielectric constant (ε_{ij}'), dielectric loss (ε_{ij}''), static dielectric constant (ε_{oij}), optical dielectric constant ($\varepsilon_{\infty ij}$) of some aprotic polar liquids in benzene at different temperatures measured under high frequency electric field of nearly 10 Ghz.

Temperature in ^{0}C	Weight fraction w_j	ε_{ij}'	ε_{ij}''	ε_{oij} at 1 KHz	$\varepsilon_{\infty ij}=n^2_{Dij}$
		DMSO in C_6H_6 at 9.174 GHz			
	0.0022	2.311	0.0280	2.3230	2.2499
	0.0043	2.342	0.0420	2.3624	2.2530
25	0.0047	2.350	0.0460	2.3731	2.2550
	0.0069	2.381	0.0616	2.4173	2.2579
	0.0086	2.414	0.0798	2.4602	2.2620
	0.0022	2.310	0.0274	2.3210	2.2470
	0.0043	2.341	0.0400	2.3610	2.2515
30	0.0047	2.348	0.0440	2.3720	2.2500
	0.0069	2.370	0.0526	2.4045	2.2545
	0.0086	2.390	0.0648	2.4362	2.2560
	0.0022	2.290	0.0234	2.2993	2.2300
	0.0043	2.312	0.0330	2.3400	2.2320
35	0.0047	2.316	0.0360	2.3470	2.2335
	0.0069	2.350	0.0496	2.3960	2.2396
	0.0086	2.370	0.0580	2.4270	2.2440
	0.0022	2.270	0.0170	2.2849	2.2201
	0.0043	2.302	0.0282	2.3300	2.2246
40	0.0047	2.304	0.0286	2.3350	2.2256
	0.0069	2.338	0.0420	2.3838	2.2297
	0.0086	2.350	0.0500	2.4120	2.2345
		DEF in C_6H_6 at 9.695 GHz			
	0.0023	2.2780	0.0256	2.3067	2.0939
30	0.0042	2.2900	0.0288	2.3336	2.1141
	0.0079	2.3140	0.0384	2.3965	2.1543
	0.0095	2.3260	0.0448	2.4208	2.1727
		DMF in C_6H_6 at 9.987 GHz			
	0.0027	2.324	0.0256	2.3446	2.2498
25	0.0036	2.339	0.0302	2.3680	2.2518
	0.0048	2.359	0.0386	2.3968	2.2545
	0.0063	2.387	0.0484	2.4434	2.2579
		DMA in C_6H_6 at 9.987 GHz			
	0.0026	2.3250	0.0213	2.3633	2.2432
25	0.0045	2.3475	0.0278	2.3988	2.2429
	0.0056	2.3625	0.0330	2.4278	2.2427
	0.0066	2.3795	0.0381	2.4508	2.2425

w_j's of solutes [3.14] (Table 3.1). The slopes a_1's of X_{ij}–w_j curves of Fig.3.5 were then used to calculate static dipole moment μ_s. All the μ_s's together with the slopes of X_{ij}–w_j curves are placed in Table 3.5. The μ_s's of Table 3.5 when compared with μ_2 and μ_1 of Table 3.4 shows that μ_s agrees with μ_1. The conformational structures of molecules in Fig.3.6 were obtained from μ_{cal} in terms of reduced bond moments by a factor μ_s/μ_{theo} in order to take into account of the mesomeric and inductive effects of the substituent polar groups [3.14]. The theoretical dipole moment μ_{theo}'s of

polar molecules are, however, derived from the available bond moments and bond angles of polar groups of the parent molecules.

3.2. Experimental Set Up :

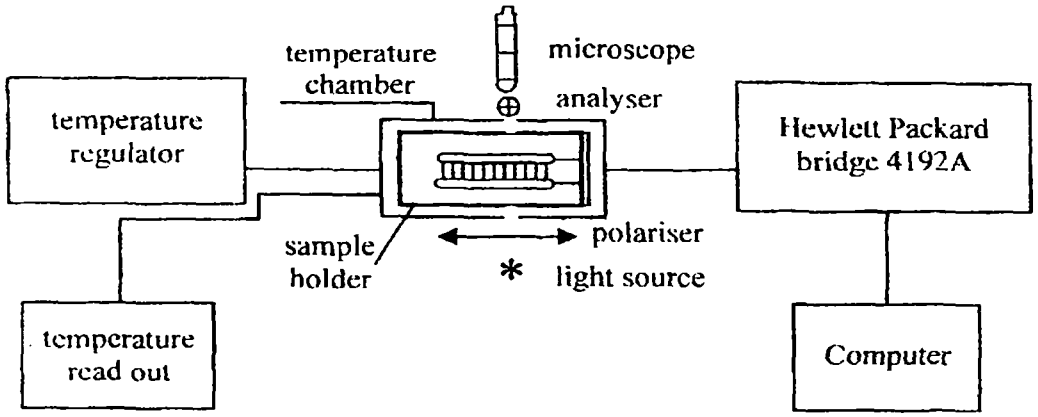

Figure A : Block diagram of the experimental setup used for dielectric measurements

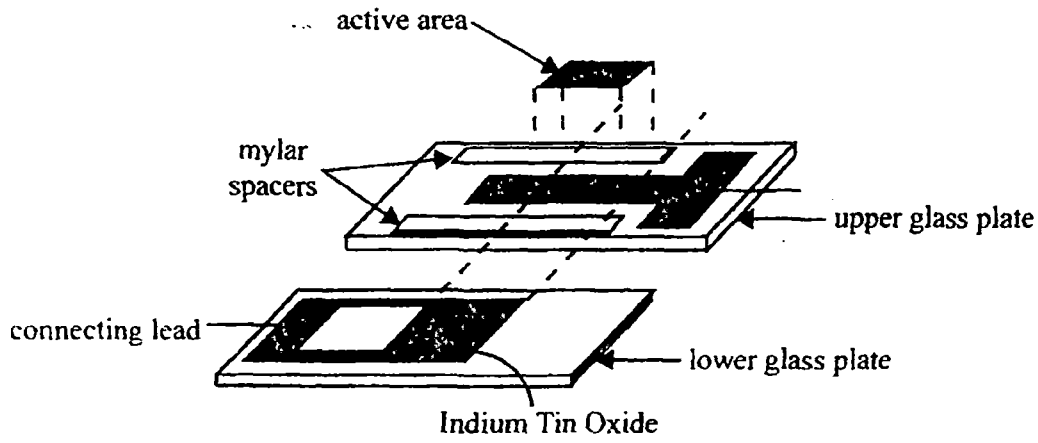

Figrure B : Inner surfaces of the lower and upper conducting glass plates.

The Block diagram for the measurement of dielectric relaxation solution (ij) data and experimental details [3.7] has been shown in the adjoining Fig.A. It consists of sample holder, temperature chamber, temperature controller and a Hewlett Packard Bridge 4192A. A cell (Fig.B) with a sample holder consists of two glass plates coated with conducting Indium Tin Oxide (ITO) in their inner surfaces. They are separated by Mylar spacer of 40 micro metre thicknesses and kept on temperature chamber Mettler Hot Stage FP 52.

The Hewlett Packard Impedance Analyser (HP 4192A) measures the complex impedance of the cell to evaluate capacitance and conductance values. Air capacitance C_0 of the cell can be written as:

$$C_o = C_L + C_S \qquad \text{.....(3.1)}$$

where C_L is the capacitance of the empty cell excluding stray capacitance C_S. When the cell is filled with the sample of known dielectric constant ε_{ij} the measured capacitance will be:

$$C = \varepsilon_{ij} C_L + C_S \qquad \text{.....(3.2)}$$

The real part of the dielectric permittivity of the sample is given by:

$$\varepsilon'_{ij} = \frac{(C - C_S)}{(C_o - C_S)} \qquad \text{.....(3.3)}$$

The dielectric loss due to absorbtion is

$$\varepsilon''_{ij} = \frac{G_{ij}}{2\pi f C_o} \qquad \text{.....(3.4)}$$

where G_{ij} and f are conductance of the solutions and frequency of the electric field.

The ITO electrode in GHz does not yield dielectric properties of the solution but rather those of the electrode materials because ITO is not sufficiently a good conductor and appropriate only upto a few MHz. The frequency range of the instrument HP 4192A was 5Hz to 13 MHz. ε_{ij}' and ε_{ij}'' for a given w_j of solute under a few MHz frequencies were carefully measured to construct the Cole-Cole semicircular arc. Both $\varepsilon_{\infty ij}$ and ε_{oij} were then accurately obtained along with ε_{ij}' and ε_{ij}'' within 5% accuracies at nearly 10 GHz to report in Table 3.1. The frequencies as quoted in Table 3.1 were found out from $(d\varepsilon_{ij}''/df)=0$ in $\varepsilon_{ij}''=a+bf+cf^2$ at which ε_{ij}' were again located. $\varepsilon_{\infty ij}$ and ε_{oij} were also verified by Abbe's refractometer and HP 4192A at 1KHz within 1% accuracy.

The solvent C_6H_6 (Spec.pure) and aprotic liquids like DMSO, DMF, DEF and DMA (E Merck, Bombay) were used after distillation. The solutions of different concentrations were made by mixing a certain weight of solute in a solvent of known weight. They were kept in dried and clean capsules for the measurement.

3.3. Theoretical Formulations :

3.3.1. Relaxation Times τ_2 and τ_1 :

The dielectric relaxation parameters under GHz electric field for two mutually independent Debye type dispersions [3.11] can be given by:

$$\frac{\varepsilon'_{ij}-\varepsilon_{\infty ij}}{\varepsilon_{oij}-\varepsilon_{\infty ij}}=c_1\frac{1}{1+\omega^2\tau_1^2}+c_2\frac{1}{1+\omega^2\tau_2^2} \qquad \ldots\ldots(3.5)$$

$$\frac{\varepsilon''_{ij}}{\varepsilon_{oij}-\varepsilon_{\infty ij}}=c_1\frac{\omega\tau_1}{1+\omega^2\tau_1^2}+c_2\frac{\omega\tau_2}{1+\omega^2\tau_2^2} \qquad \ldots\ldots(3.6)$$

Here c_1 and c_2 are the relative contributions towards dielectric relaxations due to τ_1 and τ_2 respectively.

Substituting $(\varepsilon_{ij}'-\varepsilon_{\infty ij})/(\varepsilon_{oij}-\varepsilon_{\infty ij})=x$, and $\varepsilon_{ij}''/(\varepsilon_{oij}-\varepsilon_{\infty ij})=y$, Eqs.(3.5) and (3.6) become:

$$x=c_1a_1+c_2a_2 \qquad \ldots\ldots(3.7)$$

$$y=c_1b_1+c_2b_2 \qquad \ldots\ldots(3.8)$$

where $a=1/(1+\alpha^2)$, $b=\alpha/(1+\alpha^2)$ and $\omega\tau=\alpha$. The suffices *1* and *2* with a and b are related to τ_1 and τ_2 respectively. Solving Eqs.(3.7) and (3.8) one gets:

$$c_1=\frac{(x\alpha_2-y)(1+\alpha_1^2)}{\alpha_2-\alpha_1} \qquad \ldots\ldots(3.9)$$

$$c_2=\frac{(y-x\alpha_1)(1+\alpha_2^2)}{\alpha_2-\alpha_1} \qquad \ldots\ldots(3.10)$$

provided $\alpha_2-\alpha_1\neq 0$ and $\alpha_2>\alpha_1$. Now, using $c_1+c_2=1$; one gets from Eqs.(3.9) and (3.10)

$$\frac{\varepsilon_{oij}-\varepsilon'_{ij}}{\varepsilon'_{ij}-\varepsilon_{\infty ij}}=\omega(\tau_1+\tau_2)\frac{\varepsilon''_{ij}}{\varepsilon'_{ij}-\varepsilon_{\infty ij}}-\omega^2\tau_1\tau_2 \qquad \ldots\ldots(3.11)$$

which is a straight line of $(\varepsilon_{oij}-\varepsilon_{ij}')/(\varepsilon_{ij}'-\varepsilon_{\infty ij})$ against $\varepsilon_{ij}''/(\varepsilon_{ij}'-\varepsilon_{\infty ij})$ with intercept $-\omega^2\tau_1\tau_2$ and slope $\omega(\tau_1+\tau_2)$. Here ω=angular frequency of the applied electric field of frequency f in GHz. The Eq.(3.11) is fitted with the measured ε_{ij}', ε_{ij}'', ε_{oij} and $\varepsilon_{\infty ij}$ of Table 3.1 for each aprotic polar liquid in C_6H_6 for different w_j's at a given temperature T K. The slope and intercept were used to

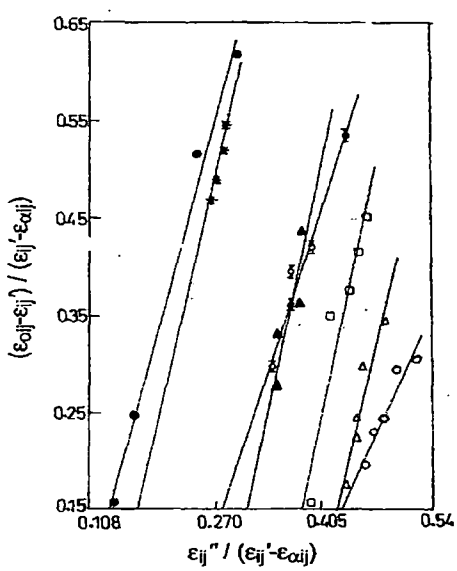

Figure 3.1: Variation of $(\varepsilon_{oij}-\varepsilon_{ij}')/(\varepsilon_{ij}'-\varepsilon_{\alpha ij})$ against $\varepsilon_{ij}''/(\varepsilon_{ij}'-\varepsilon_{\alpha ij})$ for different weight fraction w_j of some aprotic polar liquids in benzene.

DMSO (–O–,–Δ–,–□–,–Ω–) at 25°C, 30°C, 35°C, and 40°C respectively; DEF (–●–) at 30°C; DMF (–▲–) at 25°C; DMA (–✶–) at 25°C.

yield τ_1 and τ_2 as shown in Table 3.2, with the reported τ [3.5].

Table 3.2: The estimated intercepts and slopes of straight line equation of $(\varepsilon_{oij}-\varepsilon_{ij}')/(\varepsilon_{ij}'-\varepsilon_{\infty ij})$ against $\varepsilon_{ij}''/(\varepsilon_{ij}'-\varepsilon_{\infty ij})$, Correlation coefficients (r), % of error involved in regression technique, the most probable relaxation time $\tau_o=\sqrt{\tau_1\tau_2}$, and reported τ of some non-spherical aprotic polar liquids under *hf* electric field of nearly 10 GHz.

System with sl. no	Temp in ^{0}C	Intercepts and slopes of Eq.(3.11)		Correl. Coeff 'r'	% of error	Estimated values of τ_2 and τ_1 in p-secs		$\tau_o=\sqrt{\tau_1\tau_2}$	Reported τ in p sec (GK Method)
(I)DMSO in C_6H_6 M_j=78 gm	25	0.5671	1.6817	0.9605	2.34	21.08	8.10	13.07	5.37
(II)DMSO in C_6H_6 M_j=78 gm	30	1.3024	3.4358	0.9429	3.35	52.11	7.53	19.81	4.96
(III)DMSO in C_6H_6 M_j=78 gm	35	1.2899	3.8162	0.9377	3.64	59.73	6.51	19.72	4.70
(IV)DMSO in C_6H_6 M_j=78 gm	40	0.5376	2.4880	0.9862	0.83	39.04	4.15	12.73	4.33
(V)DEF in C_6H_6 M_j=101.15 gm	30	0.2592	3.0829	0.9933	0.45	49.21	1.42	8.36	2.42
(VI)DMF in C_6H_6 M_j=73 gm	25	1.0183	3.8186	0.8896	7.03	56.28	4.60	16.09	5.09
(VII)DMA in C_6H_6 M_j=87 gm	25	0.4936	3.7032	0.9011	6.34	56.81	2.21	11.20	6.53

Fröhich's theory of dielectric relaxation is based on the concept of a distribution of relaxation times with a minimum τ_1 and a maximum τ_2 values. The double relaxation method is, however, concerned with these two discrete relaxation times as the limiting values of Fröhlich's theory [3.12]. c_1 and c_2 towards dielectric relaxations are, therefore, calculated from the theoretical formulations of x and y of Fröhlich [3.12].

$$x=\frac{\varepsilon_{ij}'-\varepsilon_{\infty ij}}{\varepsilon_{oij}-\varepsilon_{\infty ij}}=1-\frac{1}{2A}\ln\left(\frac{1+e^{2A}\omega^2\tau_s^2}{1+\omega^2\tau_s^2}\right) \qquad \ldots\ldots(3.12)$$

$$y=\frac{\varepsilon_{ij}''}{\varepsilon_{oij}-\varepsilon_{\infty ij}}=\frac{1}{A}\left[\tan^{-1}(e^A\omega\tau_s)-\tan^{-1}(\omega\tau_s)\right] \qquad \ldots\ldots(3.13)$$

and are shown in Table 3.3. Here τ_S =small limiting relaxations time $=\tau_1$ and A = Fröhlich parameter $=\ln(\tau_2/\tau_1)$. 'A' is a constant which can be expressed in terms of the difference in activation energies E_2 and E_1 of a rotating unit at a given temperature because $\tau_2/\tau_1=\exp[(E_2-E_1)/k_BT]$ where k_B is the

Boltzmann constant. The values of x and y at $w_j \rightarrow 0$ from the graphical plots of Figs.3.2 and 3.3 can also be had to get c_1 and c_2. The L.H.S. of Bergmann's equatioins [3.11] are fixed for once estimated τ_1 and τ_2 from the intercept and slope of Eq.(3.11).

Table 3.3: Fröhlich parameter A, relative contributions c_1 and c_2 due to τ_1 and τ_2, theoretical values of x and y due to Fröhlich Eqs.(3.12) and (3.13) and those by graphical method at infinite dilution for some aprotic polar liquids at different and single temperature under *hf* electric field.

System with sl. no	Temp in ^{0}C	Fröhlich para meter A	Theoretical values of x and y from Eqs.(3.12) and (3.13)		Theoretical values of c_1 and c_2 from Eqs.(3.9) and (3.10)		Estimated values of x and y at $w_j \rightarrow 0$ from Figs.3.2 and 3.3		Estimated values of c_1 and c_2 from graphical technique	
			x	y	c_1	c_2	x	y	c_1	c_2
(I) DMSO in C_6H_6	25	0.9565	0.629	0.466	0.486	0.569	0.892	0.363	1.174	-0.178
(II) DMSO in C_6H_6	30	1.9345	0.449	0.434	0.423	0.934	0.900	0.338	1.094	-0.206
(III) DMSO in C_6H_6	35	2.2165	0.454	0.419	0.425	1.043	0.834	0.295	0.958	-0.075
(IV) DMSO in C_6H_6	40	2.2415	0.610	0.409	0.507	0.794	0.848	0.225	0.885	0.067
(V) DEF in C_6H_6	30	3.5454	0.677	0.328	0.588	0.924	0.988	0.055	1.006	-0.104
(VI) DMF in C_6H_6	25	2.5043	0.497	0.405	0.451	1.086	0.872	0.210	0.959	-0.173
(VII) DMA in C_6H_6	25	3.2467	0.600	0.357	0.530	1.096	0.736	0.126	0.743	0.096

3.3.2. High Frequency Dipole Moments μ_1, μ_2 of τ_1, τ_2 :

The high frequency complex conductivity σ_{ij}^* of liquid mixture is expressed by $\sigma_{ij}^* = \sigma_{ij}' + j\sigma_{ij}''$ while the total conductivity is

$$\sigma_{ij} = \frac{\omega}{4\pi}\left(\varepsilon_{ij}'^2 + \varepsilon_{ij}''^2\right)^{1/2} \qquad \ldots\ldots (3.14)$$

as a function of w_j. Although ε_{ij}'' offers resistance to polarisation, still in the *hf* region $\varepsilon_{ij}' \gg \varepsilon_{ij}''$.

The real part of *hf* conductivity is [3.13]:

$$\sigma_{ij}' = \frac{N\rho_{ij}\mu_j^2 F_{ij}}{3k_B T M_j}\left(\frac{\omega^2\tau}{1+\omega^2\tau^2}\right)w_j$$

which on differentiation with respect to w_j and at $w_j \to 0$ yields:

$$\left(\frac{d\sigma'_{ij}}{dw_j}\right)_{w_j \to 0} = \frac{N\rho_i \mu_j^2 F_i}{3k_B T M_j}\left(\frac{\omega^2\tau}{1+\omega^2\tau^2}\right) \qquad \ldots\ldots(3.15)$$

where F_{ij}=the local field of the solution=$(\varepsilon_{ij}+2)^2/9$. F_{ij} Becomes F_i and ρ_{ij} tends to ρ_i at $w_j \to 0$, where $F_i=(\varepsilon_i+2)^2/9$. ε_i and ρ_i are the dielectric constant and density of the solvent respectively. The other symbols carry usual significance [3.9-3.10].

Again, since $\sigma_{ij}=(\omega\varepsilon_{ij}'/4\pi)$ we have

$$\sigma_{ij} = \sigma_{\infty ij} + \frac{1}{\omega\tau}\sigma'_{ij}$$

or,

$$\left(\frac{d\sigma'_{ij}}{dw_j}\right)_{w_j \to 0} = \omega\tau\left(\frac{d\sigma_{ij}}{dw_j}\right)_{w_j \to 0} = \omega\tau\beta \qquad \ldots\ldots(3.16)$$

where β is the slope of σ_{ij}–w_j curve at $w_j \to 0$.

Table 3.4: The estimated coefficients α, β and γ of σ_{ij}–w_j curves (Fig.3.4), dimensionless parameters b_2 and b_1, dipole moments μ_j's in Debye of some non-spherical aprotic polar liquids in benzene under *hf* electric field of nearly 10 GHz at single and different temperatures.

System with sl. no. & mol. wt.	Temp. in ^{0}C	Coefficients α, β and γ of $\sigma_{ij} \times 10^{-10}=\alpha+\beta w_j+\gamma w_j^2$ in $\Omega^{-1}cm^{-1}$			Dimensionless parameters		Estimated dipole moments in Debye		Reported μ_j in Debye
					b_2	b_1	μ_2	μ_1	
(I) DMSO in C_6H_6 M_j=78 gm	25	1.047	5.649	157.35	0.4040	0.8212	4.67	3.28	3.79
(II) DMSO in C_6H_6 M_j=78 gm	30	1.043	8.180	-231.74	0.0999	0.8416	11.47	3.95	3.83
(III) DMSO in C_6H_6 M_j=78 gm	35	1.040	4.158	164.83	0.0779	0.8767	9.38	2.80	4.04
(IV) DMSO in C_6H_6 M_j=78 gm	40	1.023	8.897	-274.83	0.1650	0.9459	9.55	3.99	4.11
(V) DEF in C_6H_6 M_j=101.15 gm	30	1.098	2.839	32.45	0.1002	0.9926	7.47	2.38	3.88
(VI) DMF in C_6H_6 M_j=73 gm	25	1.141	6.544	245.95	0.0743	0.9232	10.88	3.09	3.62
(VII) DMA in C_6H_6 M_j=87 gm	25	1.153	1.884	533.11	0.0729	0.9811	6.43	1.75	3.37

From Eqs.(3.15) and (3.16) one gets

$$\mu_j = \left(\frac{27 k_B T M_j}{N \rho_i (\varepsilon_i + 2)^2} \frac{\beta}{\omega b} \right)^{1/2} \quad \ldots\ldots (3.17)$$

in order to obtain μ_1 or μ_2 in terms of b_1 and b_2 where b_1 and b_2 are the dimensionless parameters involved with τ_1 and τ_2 i.e,

$$b_1 = \frac{1}{1+\omega^2 \tau_1^2} \text{ and } b_2 = \frac{1}{1+\omega^2 \tau_2^2} \quad \ldots\ldots (3.18)$$

Both b_1 and b_2 as well as the coefficients α, β and γ of σ_{ij}– w_j equations in Fig.3.4 are shown in Table 3.4 together with μ_1 and μ_2 of the flexible part and the whole molecule of a polar liquid.

Table 3.5: Coefficients a_o, a_1 and a_2 in equation $X_{ij}=a_o+a_1 w_j+a_2 w_j^2$. static dipole moment μ_s in Debye and theoretical dipole moment μ_{theo} by considering inductive and mesomeric moments of substituent polar group of some aprotic polar liquids in benzene.

System with sl. no. & mol. wt.	Temp in ^{0}C	Coefficients a_o, a_1 and a_2 of $X_{ij} = a_o + a_1 w_j + a_2 w_j^2$			μ_s in Debye	μ_{theo} in Debye	μ_{cal} in Debye (corrected)	μ_s/μ_{theo}
(I) DMSO in C_6H_6 M_j= 78 gm	25	0.0022	0.7756	20.935	3.19	4.55	3.20	0.70
(II) DMSO in C_6H_6 M_j= 78 gm	30	0.0019	1.0315	-17.183	3.72	4.55	3.72	0.82
(III) DMSO in C_6H_6 M_j= 78 gm	35	0.0018	0.9346	0.000	3.58	4.55	3.58	0.79
(IV) DMSO in C_6H_6 M_j= 78 gm	40	0.0010	1.1913	-23.282	4.08	4.55	4.08	0.90
(V) DEF in C_6H_6 M_j= 101.15 gm	30	0.0116	0.2047	0.000	1.89	3.99	1.89	0.47
(VI) DMF in C_6H_6 M_j= 73 gm	25	0.0028	0.7301	61.438	2.99	3.82	2.99	0.78
(VII) DMA in C_6H_6 M_j= 87 gm	25	0.0044	0.6545	53.798	3.09	4.02	3.09	0.77

3.3.3. Static Dipole Moments :

The Debye equation for a polar nonpolar liquid mixture of w_j of a polar liquid under static or low frequency electric field at a given T K is [3.14].

$$\frac{\varepsilon_{oij} - n_{Dij}^2}{(\varepsilon_{oij}+2)(n_{Dij}^2+2)} = \frac{\varepsilon_{oi} - n_{Di}^2}{(\varepsilon_{oi}+2)(n_{Di}^2+2)} + \frac{4\pi N \mu_s^2 \rho_i}{27 k_B T M_j} w_j (1-\gamma w_j)^{-1}$$

or,

$$X_{ij} = X_i + \frac{4\pi N\mu_s^2\rho_i}{27k_BTM_j}w_j + \frac{4\pi N\mu_s^2\rho_i}{27k_BTM_j}\gamma w_j^2 + \ldots\ldots \qquad \ldots\ldots (3.19)$$

where X_{ij} and X_i are the static experimental parameters of the solution and solvent. $\gamma=(1-\rho_i/\rho_j)$, ρ_i and ρ_j are densities of pure solvent and solute respectively. The usual variation of X_{ij} with w_j is of the form:

$$X_{ij} = a_o + a_1 w_j + a_2 w_j^2 \qquad \ldots\ldots (3.20)$$

satisfying the experimental curves of Fig.3.5. The coefficients a_0, a_1 and a_2 of Eq.(3.20) with the measured data of Table 3.1 were, however, calculated and are placed in Table 3.5. Equating the first power of w_j of Eqs.(3.19) and (3.20) and neglecting terms of higher powers of w_j for their involvement with various interactions [3.14] one gets the static μ_s from:

$$\mu_s = \left(\frac{27k_BTM_j}{4\pi N\rho_i}a_1\right)^{1/2} \qquad \ldots\ldots (3.21)$$

in order to present them in Table 3.5 for comparison with μ_1 and μ_2 of Table 3.4 in terms of τ_1 and τ_2.

3.4. Results and Discussions :

The variations of experimental $(\varepsilon_{oij}-\varepsilon_{ij}')/(\varepsilon_{ij}'-\varepsilon_{\infty ij})$ with $\varepsilon_{ij}''/(\varepsilon_{ij}'-\varepsilon_{\infty ij})$ at different w_j's of solutes displayed in Fig.3.1 on fitted lines are derived to be linear as predicted by Eq.(3.11). The slopes and intercepts of Eq.(3.11) for aprotic polar liquids in C_6H_6 are presented in Table 3.2 along with the estimated τ_2 and τ_1. The linear variation is supported by the correlation coefficient 'r' and the corresponding % of errors placed in Table 3.2 in getting the straight lines of Fig.3.1. The errors within 10% indicate probably the accurate measurements of data of Table 3.1.

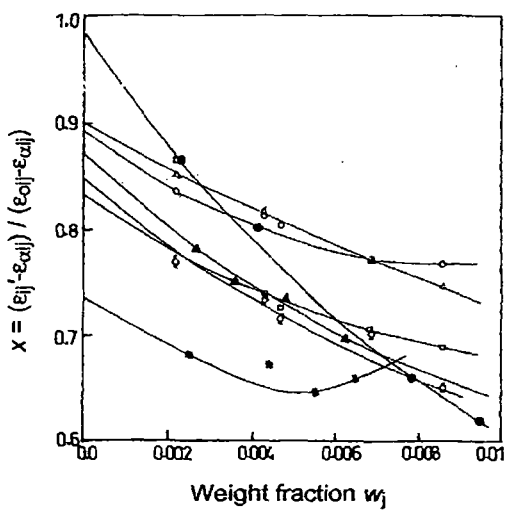

Figure 3.2: Variation of measured $x=(\varepsilon_{ij}'-\varepsilon_{\infty ij})/(\varepsilon_{oij}-\varepsilon_{\infty ij})$ with w_j of some aprotic polar liquids.

DMSO (–O–,–Δ–,–□–,–Ω–) at 25°C, 30°C, 35°C, and 40°C respectively; DEF (–●–) at 30°C; DMF (–▲–) at 25°C; DMA (–✶–) at 25°C

It is evident from Fig.3.1 that all the straight lines of DMSO in C_6H_6 shift towards the origin as the temperature increases from 25°C to 40°C. This sort of behaviour of DMSO invites a further study to see the existence of single relaxation at higher temperature. So, like electric field frequency (*f*), temperature is also a factor for such behaviour of molecules [3.10]. All the liquids show double relaxation times τ_2 and τ_1 as evident from the negative intercepts of the curves. τ_1's of the molecules [3.2-3.3] agree well with the reported τ in Table 3.2 due to Gopalakrishna's method [3.15-3.16]. It signifies that the electric field of 10 GHz frequency is the most effective dispersive region [3.6] for probable rotations of the flexible parts of these molecules [3.14]. Unlike τ_1's of DMSO; τ_2's are found to increase with temperature. The linear equation of $\ln(\tau_1 T)$ and $\ln(\tau_2 T)$ with $1/T$ were found out by [3.17]:

$$\ln(\tau_1 T) = -32.1273 + 3.6861 \times 10^3 (1/T)$$

$$\ln(\tau_2 T) = -4.8261 - 4.0995 \times 10^3 (1/T)$$

Indicating that τ_1 obeys Eyring's rate process. The energy parameters like enthalpy of activation ΔH_{τ_1}=7.32 Kcal/mole and ΔH_{τ_2} = −8.13 Kcal/mole; entropy of activation ΔS_{τ_1} are 16.79, 16.50, 16.36, 16.84 Cal/mole/K and ΔS_{τ_2} are −36.96, −38.34, −38.21, −36.98 Cal/mole/K. The corresponding free energy of activation ΔF_{τ_1} and ΔF_{τ_2} are 2.32, 2.32, 2.28, 2.05 and 2.88, 3.49, 3.64, 3.44 Kcal/mole at 25°, 30°, 35° and 40°C respectively. The data thus obtained confirm the whole molecular rotation under 10 GHz electric field as a cooperative process while the reverse is true for rotation of the flexible group.

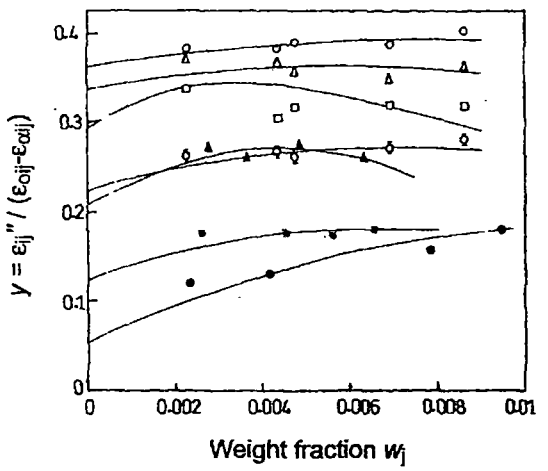

Figure 3.3: Variation of measured $y = \varepsilon_{ij}''/(\varepsilon_{oij} - \varepsilon_{\infty ij})$ with w_j of some aprotic polar liquids.

DMSO (–O–,–Δ–,–□–,–Q–) at 25°C, 30°C, 35°C, and 40°C respectively; DEF (–●–) at 30°C; DMF (–▲–) at 25°C; DMA (–✶–) at 25°C

The increase of τ_2 with the rise of temperature is due to elongation of size for monomer [3.18] formation with C_6H_6 (see Fig.3.6).

For aprotic polar molecules of greater complexity where a few experimental data are available under a single frequency electric field (Table 3.1) a continuous distribution of τ between two limiting values could be used [3.11]. The c_1 and c_2 values towards dielectric relaxations in terms of estimated τ_1 and τ_2 were, therefore, calculated from x and y of Fröhlich's Eqs.(3.12) and (3.13)

based on distribution of relaxation times. They were also obtained from $x=(\varepsilon_{ij}'-\varepsilon_{\infty ij})/(\varepsilon_{oij}-\varepsilon_{\infty ij})$ and $y=\varepsilon_{ij}''/(\varepsilon_{oij}-\varepsilon_{\infty ij})$ at $w_j\rightarrow 0$ from the graphical plots of Figs.3.2 and 3.3 as presented in Table 3.3. The explanation of the nature of variation of x and y with w_j in Figs.3.2 and 3.3 is that τ increases with w_j [3.19] the R.H.S. of Bergmann's Eqs.(3.5) and (3.6) become concave and convex cutting the ordinate axes to yield x and y respectively at $w_j\rightarrow 0$. As seen from Table 3.3; c_1 and c_2 for Fröhlich's method are positive in almost all cases. But c_2 is negative for graphical method probably due to the inertia of the flexible parts of the polar groups of the molecules [3.9].

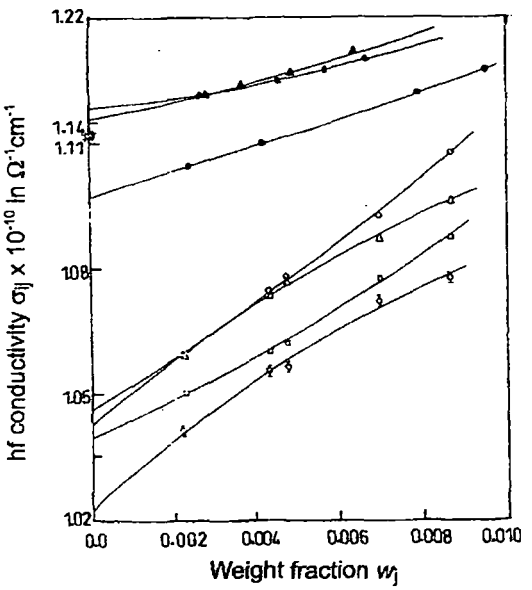

Figure 3.4: Variation of σ_{ij} with w_j of polar liquids.

DMSO (–O–,–Δ–,–□–,–Q–) at 25°C, 30°C, 35°C, and 40°C respectively; DEF (–●–) at 30°C; DMF (–▲–) at 25°C; DMA (–✶–) at 25°C

The values of μ_2 and μ_1 in terms of b's involved with τ_2's, τ_1's and slopes β's of σ_{ij}–w_j curves of Fig.3.4 were estimated from Eq.(3.17) and placed in Table 3.4. The variation of σ_{ij} with w_j are parabolic governed by α, β and γ coefficients probably due to solute-solvent associations [3.2-3.3]. The polar liquid in a given nonpolar solvent behaves as a bound charged species due to polarisation under GHz electric filed in order to have very large conductivity σ_{ij} of the order of 10^{10} $\Omega^{-1}cm^{-1}$ for different w_j's although they are insulators. They are found to decrease with the rise of temperature for DMSO for the presence of $(\rho_i F_i/T)$ in Eq.(3.15) in the limit $w_j=0$ [3.20]. It is interesting to note that μ_1 due to flexible part of the molecule agree well with the reported μ's [3.2-3.3] of Gopalakrishna's method [3.15-3.16]. This indicates that a part of the molecule is rotating under GHz electric field [3.14]. μ_2's are found to be higher in magnitudes for larger values of τ_2's according to Eq.(3.17). Both μ_2 and μ_1 vary with temperature in °C for DMSO in C_6H_6.

$$\mu_2 = -67.35 + 4.56t - 0.066t^2$$

$$\mu_1 = 8.20 - 0.32t + 0.005t^2$$

μ_2 of the parent molecule attains maximum value of 11.41 D at 34.5°C with zero dipole moments at 21.4°C and 47.7°C respectively due to monomer formation [3.2-3.3] with C_6H_6 ring (see Fig.3.6).

The degree of solubility of solutions was kept fairly constant at all temperatures and for the low concentrations of binary mixtures (Table 3.1), dimer formation [3.1-3.4] is not expected. μ_I on the other hand, decreases to a minimum value of 3.08 D at 32°C exhibiting the dimer formation of the flexible parts of their active involvement in rotation under 10 GHz electric field, unlike the whole molecule.

The static μ_s's of these liquids are also calculated from Eq.(3.21) with the measured data (Table 3.1) in terms of linear coefficients a_1's of the static experimental parameter X_{ij} against w_j curves of Fig.3.5. The coefficients a_0, a_1 and a_2 of the curves with the estimated μ_s are presented in Table 3.5. All the curves are found to be of almost same intercepts and slopes for DMSO in C_6H_6 at different temperatures signifying the fact that the static polarisability is nearly constant at all temperatures. The curves of X_{ij}–w_j in case of DMF and DMA at 25°C are, however, parabolic in nature probably due to the presence of the substituent –CH_3 group attached to the parent molecules under identical environment. But X_{ij} varies with w_j linearly in case of DEF at 30°C. All these curves in Fig.3.5 with the computed μ_s's suggest that the measured data of Table 3.1 are more than accurate.

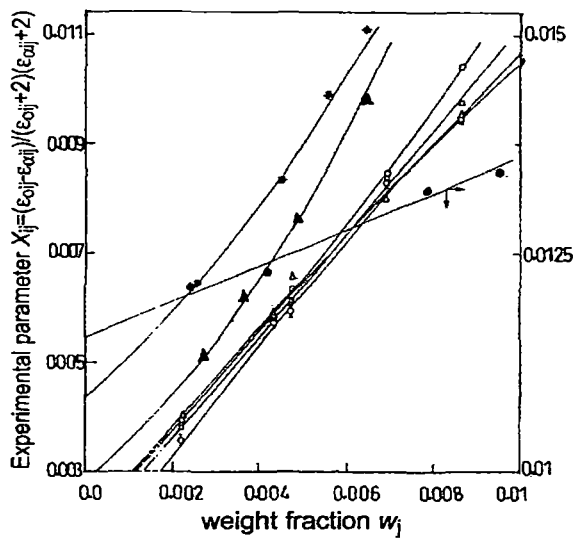

Figure 3.5: Variation of the measured X_{ij} with w_j of some aprotic polar liquids.

DMSO (–O–,–Δ–,–□–,–Ω–) at 25°C, 30°C, 35°C, and 40°C respectively; DEF (–●–) at 30°C; DMF (–▲–) at 25°C; DMA (–✶–) at 25°C

The theoretical μ_{theo}'s of polar molecules assumed to be planer ones were defined by the vector addition of the available bond moments 2.35D, 1.55D for polar groups S←CH_3, O⇐S in DMSO; 0.64D, 0.78D, 0.37D of N←CH_3, N←C_2H_5, CH_3←C in DMF, DEF and DMA. The other common bond moments are 0.3D, 0.45D, 3.10D for C←H, C←N and C⇐O respectively in them. The N atoms in DMF, DEF, DMA and S atom in DMSO molecules are thought to be slightly fractional positively charged δ^+ with benzene to make monomer formations [3.2-3.3]. The solute-solvent molecular association arises from the interaction of the π-delocalised electron cloud of the benzene ring with the fractional positive charges δ^+ on the N and S atoms of the amide groups. The bond moments of polar groups under the static and high frequency electric field are, however,

reduced by a factor μ_s/μ_{theo} in the range 0.5 and 0.9 due to inductive and mesomeric effects to yield μ_{cal} in agreement with μ_s. μ_s/μ_{theo} thus appears to exhibit the material property of the systems. The conformational structures of the polar molecules with their monomer [3.2-3.3] associations in C_6H_6 are shown in Fig.3.6. μ_{theo}'s along with μ_{cal} and μ_s/μ_{theo} are placed in Table 3.5 for comparison.

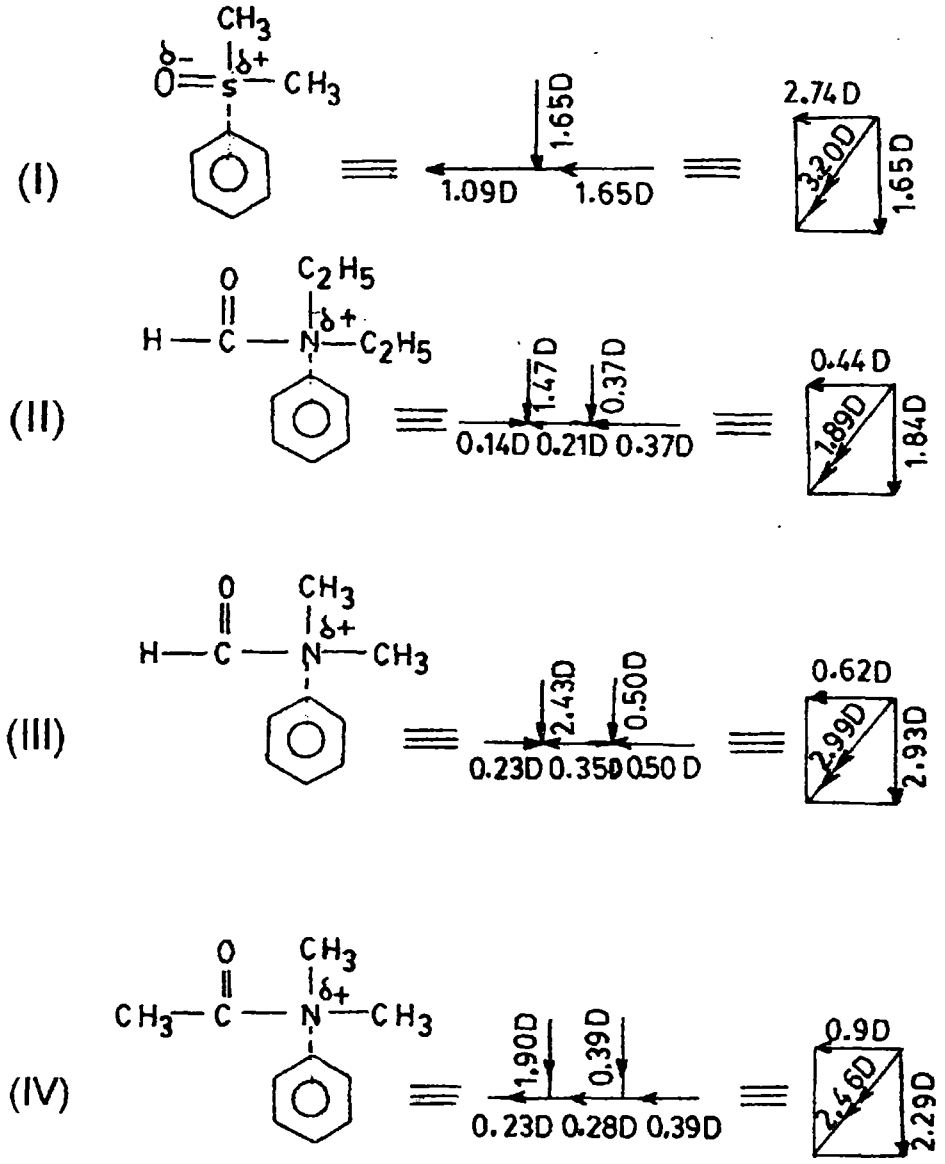

Figure 3.6: Conformational structures of aprotic polar liquids in terms of reduced bond length due to mesomeric and inductive moments of the substituent polar groups.

(I) DMSO in C_6H_6; (II) DEF in C_6H_6; (III) DMF in C_6H_6; (IV) DMA in C_6H_6

3.5. Conclusion :

The present measurements of dielectric relaxation parameters near 10 GHz electric field at different temperatures are found to exhibit double relaxation phenomena for rigid aprotic polar liquids. The procedure in obtaining τ_2 and τ_1 from the slope and intercept of a derived linear equation with ε_{oij}, $\varepsilon_{\infty ij}$, ε_{ij}' and ε_{ij}'' measured under the single frequency electric field appears to be a significant improvement over the existing ones where data at two or more frequencies are required. The % of error in terms of correlation coefficient 'r' in getting intercept and slope is made because of the linearity of the curve. The estimated τ_2 and τ_1 of the whole and the flexible part attached to the parent molecule are reliable as τ is claimed to be accurate within ±10%. It is interesting to note that unlike τ_2, τ_1 obeys Eyring's rate theory. The relative contributions c_1 and c_2 towards dielectric relaxations due to τ_1 and τ_2 are calculated by the graphical technique at $w_j \rightarrow 0$ as well as Fröhlich's method based on the concept of a distribution of τ between τ_1 and τ_2. The μ_2 and μ_1 of the whole and the flexible part attached to the parent molecule within ±5% accuracy are obtain from the slope β of σ_{ij}– w_j curves and τ_2, τ_1. The static μ_s from the linear coefficient of X_{ij}–w_j curve when compared with μ_2 and μ_1 from high frequency absorbtion reveals that μ's are little affected by the frequency (f) of the electric field. The X_{ij}–w_j curves and μ_s's may be used to test the accuracies of relaxation parameters. It is confirmed that a part of the molecule is rotating under 10 GHz electric field. Besides 'f', temperature is a factor to show mono or double relaxation behaviour for a molecule. The conformational structures of molecules from the reduced bond moments of polar groups by a factor μ_s/μ_{theo} due to mesomeric and inductive moments in them under static or low frequency electric field are in agreement with μ_s. μ_{theo} is obtained from available bond moments of polar groups. Thus the methodology, so far advanced, seems to be simple, straightforward and useful to observe interesting phenomena of *hf* absorbtion in polar-nonpolar liquid mixture.

References :

[3.1] A K Sharma and D R Sharma, *J. Phys. Soc. Japan* **53** 4771 (1984)

[3.2] J S Dhull and D R Sharma, *Indian J. Pure & Appl. Phys.* **21** 694 (1983)

[3.3] A Sharma and D R Sharma, *J. Phys. Soc. Japan* **61** 1049 (1992)

[3.4] A R Sharma, D R Sharma and M S Chauhan, *Indian J. Pure & Appl. Phys.* **31** 841 (1993)

[3.5] K V Gopalakrishna, *Trans. Faraday Soc.* **53** 767 (1957)

[3.6] S K Sit and S Acharyya, *Indian J. Pure & Appl. Phys.* **34** 255 (1996)

[3.7] T Pal Majumder, *Ph D Thesis* Jadavpur University, Calcutta (1996)

[3.8] K Higasi, K Bergmann and C P Smyth, *J. Phys. Chem.* **64** 880 (1960)

[3.9] U Saha, S K Sit, R C Basak and S Acharyya, *J. Phys. D: Appl. Phys.* **27** 596 (1994)

[3.10] S K Sit, R C Basak, U Saha and S Acharyya, *J. Phys. D: Appl. Phys.* **27** 2194 (1994)

[3.11] K Bergmann, D M Roberti and C P Smyth, *J. Phys. Chem.* **64** 665 (1960)

[3.12] H Fröhlich, *Theory of Dielectrics* (Oxford University Press) p.94 (1949)

[3.13] C P Smyth, *Dielectric Behaviour and Structure* (Mc Graw-Hill : New York) (1955)

[3.14] R C Basak, S K Sit, N Nandi and S Acharyya, *Indian J. Phys.* **70B** 37 (1996)

[3.15] J S Dhull and D R Sharma, *J. Phys. D: Appl. Phys.* **15** 2307 (1982)

[3.16] A R Saksena, *Indian J. Pure & Appl. Phys.* **16** 1079 (1978)

[3.17] H Eyring, S Glasstone and K J Laidler, *Theory of Rate Process* (Mc Graw-Hill : New York) (1941)

[3.18] U Saha and S Acharyya, *Indian J. Pure & Appl. Phys.* **32** 346 (1994)

[3.19] S N Sen and R Ghosh, *Indian J. Pure & Appl. Phys.* **10** 701 (1972)

[3.20] U Saha and S Acharyya, *Indian J. Pure & Appl. Phys.* **31** 181 (1993)